Available online at www.sciencedirect.com
SCIENCE DIRECT®
Polymer 44 (2003) 6003–6011
polymer
www.elsevier.com/locate/polymer

Molecular orientation and structural development in vulcanized polyisoprene rubbers during uniaxial deformation by in situ synchrotron X-ray diffraction

Shigeyuki Toki*, Igors Sics, Shaofeng Ran, Lizhi Liu, Benjamin S. Hsiao*

Department of Chemistry, State University of New York at Stony Brook, Stony Brook, NY 11794-3400, USA

Received 15 December 2002; received in revised form 2 April 2003; accepted 7 April 2003

Dedicated to Prof. Ian M. Ward on the occasion of his 75th birthday

Abstract

Molecular orientation and strain-induced crystallization of vulcanized natural rubbers (by sulfur and peroxide) and synthetic polyisoprene rubber (by sulfur) during uniaxial deformation at 0 °C were studied by in situ synchrotron wide-angle X-ray diffraction. The high intensity of synchrotron X-rays and new image analysis methods made it possible to estimate the mass fractions of strain-induced crystals and amorphous chains in both oriented and unoriented states. Most of the polymer chains (~75%) were found to be in the random coil state even at large strains (>5.0). Only about 5% the amorphous chains were oriented, whereas the rest of the chains (~20%) were in the crystalline phase. Sulfur vulcanized and peroxide vulcanized natural rubbers did not exhibit notable differences in structure and property relationships. In contrast, synthetic polyisoprene rubber showed a different behavior of deformation-induced structural changes, which can be attributed to the difference in cross-link topology. Our results indicated that strain induces a network of microfibrillar crystals in both natural and synthetic polyisoprene rubbers due to the inhomogeneity of cross-link distribution that is responsible for their elastic properties.

Keywords: Polyisoprene; Rubber; Deformation

1. Introduction

Vulcanized rubber under deformation has been a subject of intensive research interest since the 1940s. Several major topics in polymer science, including rubber elasticity theory and structure–property relationships in polymeric solids, were initiated from this subject [1–9]. It has been well demonstrated that the roles of both molecular orientation and strain-induced crystallization are crucial for determining the final mechanical properties of rubber [3–5,9].

The phenomenon of strain-induced crystallization in natural rubber has been extensively studied by X-ray diffraction techniques using laboratory X-ray sources [9–15]. In these studies, the stretched samples were always held for a long period of time (several hours) to accommodate the relatively weak X-ray intensity. Thus, the structures detected were in the stretched but relaxed state. Only recently, real time X-ray studies using synchrotron radiation have been carried out during in situ deformation of sulfur vulcanized natural rubber (NR-S) at room temperature (25 °C) where structural development and stress–strain relationship were measured simultaneously [16,17]. The synchrotron studies revealed several new insights into the behavior of molecular orientation and strain-induced crystallization in natural rubber under uniaxial deformation, which can be summarized as follows.

1. During deformation, up to 75% of polymer chains still remain in the unoriented state even at large strains (up to 6.0). Only around 20% of the molecules are in the crystalline state, and 5% of the molecules are in the oriented amorphous state.
2. The strain-induced crystallites are highly oriented with excellent alignment along the stretching direction.
3. The crystallization pathway and the melting pathway can be distinguished from the cyclic stress–strain relation.

* Corresponding author. Tel: +1-631-632-7793; fax: +1-631-632-6518.
E-mail addresses: stoki@mail.chem.sunysb.edu (S. Toki), bhsiao@notes.cc.sunysb.edu (B.S. Hsiao).

0032-3861/03/$ - see front matter © 2003 Published by Elsevier Ltd.
doi:10.1016/S0032-3861(03)00548-2

The hysteresis behavior of the stress–strain relation is directly related to the formation and the melting of strain-induced crystallites.

4. The inhomogeneity of cross-link topology in vulcanized natural rubber creates a microfibrillar structure composed of crystalline segments between the cross-links (vulcanized points) during stretching.

The purpose of this paper is to investigate if the above behavior is universal for other similar systems such as peroxide vulcanized natural rubber (NR-P) and sulfur vulcanized synthetic polyisoprene rubber (IR) under tensile stretching. Since the deformation-induced crystallization process also depends on the experimental temperature, we chose 0 °C to enhance the stability of the strain-induced crystallites in rubber.

There are three major differences between natural rubber (NR) and synthetic polyisoprene rubber (IR), which have been described in detail recently [18,19]. (1) NR is composed of 94% (by weight) polyisoprene, 2–3% proteins, 1–1.5% fatty acids and 1–1.5% conjugated phosphoid-lipid. In contrast, IR contains only polyisoprene molecules (100%). (2) The polyisoprene component in NR is composed of 100% *cis*-1,4 conformation, whereas the polyisoprene component in IR contains only 98.5% *cis*-1,4 conformation. (3) The polyisoprene in NR contains branched chains because their end functional groups can react with each other after polyisoprene latex has been extracted from the Hevea tree. As a result, the gel content of NR can reach a level of 50–70%. Although the content of the branched polyisoprene chains in IR is not known, it may be below 20% because the gel content of IR is usually 10–20%. In other words, the majority of the polyisoprene chains in IR are linear.

To evaluate the effect of network structures (or cross-link topology) on the behavior of deformation-induced crystallization and the corresponding mechanical properties, NR-S and NR-P were also compared. The process of peroxide vulcanization usually makes the cross-linking reaction more heterogeneous because the free radical reaction in peroxide is much faster than that in sulfur vulcanization. Since the peroxide vulcanization creates (–C–C–) bonds that have higher bond energy than that of the sulfur's bonds, the peroxide vulcanized rubber is stronger against heat and mechanical deformation than the sulfur vulcanized rubber. On the other hand, the sulfur vulcanized rubber has higher tensile strength and tear strength. This is because the sulfur bonds are composed of mono-sulfur (–S–), di-sulfur (–S–S–) and multi-sulfur (–S–S–S_m–) molecules. Sulfur vulcanized rubber is more flexible under high stress concentration and exhibits higher tensile strength through the rearrangement of three types of sulfur bonds. In this work, the strain-induced crystallization behavior of sulfur vulcanized synthetic polyisoprene rubber will also be compared to those of the vulcanized nature rubbers (by peroxide and sulfur).

2. Experimental

Synchrotron X-ray measurements were carried out at the X27C beamline in the National Synchrotron Light Source (NSLS), Brookhaven National Laboratory (BNL). The wavelength of the X-ray used was 1.37 Å. Two-dimensional wide-angle X-ray diffraction (WAXD) patterns were recorded by the MAR-CCD X-ray detector (MAR USA) for quantitative image analysis. The typical image acquisition time for each scan was 30 s. All measured WAXD images were corrected for beam fluctuations and sample absorption for data analysis.

The tensile machines allowed the symmetric stretching of the sample, which permitted the focused X-ray to illuminate the same sample position during deformation. The chosen deformation rate was 10 mm/min. The experiments were carried out at 0 °C, which was controlled by an environmental chamber. The instrument was developed by modifying a tabletop stretching machine from Instron Inc. Time-resolved WAXD patterns and simultaneous stress–strain relation were recorded continuously without holding the sample in still conditions during stretching and retraction.

The recipes and cure conditions for preparation of the rubber samples are listed in Table 1. The chosen recipe for sulfur vulcanized rubber was similar to Treloar's classic compound [3], and one for peroxide vulcanized rubber was similar to Mitchell's scheme [14]. The apparent values of the average molecular weight between the network points (Mc) were estimated from the tensile elastic modulus using the simple molecular theory of rubber elasticity [2], assuming that the cross-links were distributed homogeneously. The values are also listed in Table 1.

3. Results and discussion

The stress–strain curve and selected WAXD patterns in

Table 1
The recipes and cure conditions of vulcanized rubber samples: sulfur vulcanized NR (NR-S), sulfur vulcanized IR (IR-S), peroxide vulcanized NR (NR-P)

	NR-S	IR-S	NR-P
NR	100		100
IR		100	
Stearic acid	2.0	2.0	
Anti-oxidant	1.0	1.0	
Active ZnO	1.0	1.0	
Accelerator	1.0	1.0	
Sulfur	1.5	1.5	
Peroxide			2.0
Mc (g/mol)	5000	6100	4100

NR: SMR-L, Standard Malaysian Rubber light color. IR: IR2200, Good Year. Antioxidant, (MBMTB); Accelerator, (TBBS); Peroxide, dicumyl peroxide (DCP). Sulfur vulcanized rubber: cured at 160 °C for 60 min. Peroxide vulcanized rubber: cured at 150 °C for 50 min.

NR-S during stretching and retraction at 0 °C are shown in Fig. 1. The arrow indicates the average strain value where the image was taken. The high intensity of synchrotron X-rays made it possible to collect the WAXD patterns during deformation in real time without holding the sample still. In Fig. 1, it is seen that highly oriented crystalline reflection peaks begin to appear at a strain around 2.0. The strain-induced crystal structure is consistent with a monoclinic unit cell of polyisoprene with parameters: $a = 1.25$ nm, $b = 0.89$ nm, c (chain axis) $= 0.81$ nm, and $\beta = 92°$, which has been reported by Bunn [12]. The intensities of these reflections increase with strain during stretching and decrease upon retraction. However, the crystalline diffraction pattern during retraction is much more apparent than the one during stretching at the same strain. For example, at the strain of 1.0, no crystalline pattern is observed during stretching but clear crystalline reflections are seen during retraction. The stress–strain curve shows a hysteresis, typically found in pure vulcanized natural rubber. The stress during retraction is much smaller than the stress during stretching. This is especially the case at strains less than 3.0, where the corresponding stress during retraction is almost zero.

When the strain returns to zero, the crystalline reflections disappear completely. It suggests that the induced crystallization is completely reversible even at 0 °C. The amorphous halo is found to persist in WAXD during both processes of stretching and retraction (even at the highest applied strain of 5). Compared to our previous results from the same sample at 25 °C, the observed starting strain for crystallization is smaller and the strain due to melting is smaller at 0 °C [17]. In general, the hysteresis of the stress–strain curve and the effect of strain-induced crystallization on the mechanical properties is much larger at 0 °C than at 25 °C.

Time-resolved WAXD patterns and the simultaneously measured stress–strain curve of NR-P at 0 °C is shown in Fig. 2. The behavior seems to be very similar to that of NR-S. In general, the stress of NR-P shows a much higher value than the corresponding stress of NR-S under the same strain conditions. It is interesting to see that the stress during retraction reaches almost zero at strains below 3.0, similar to

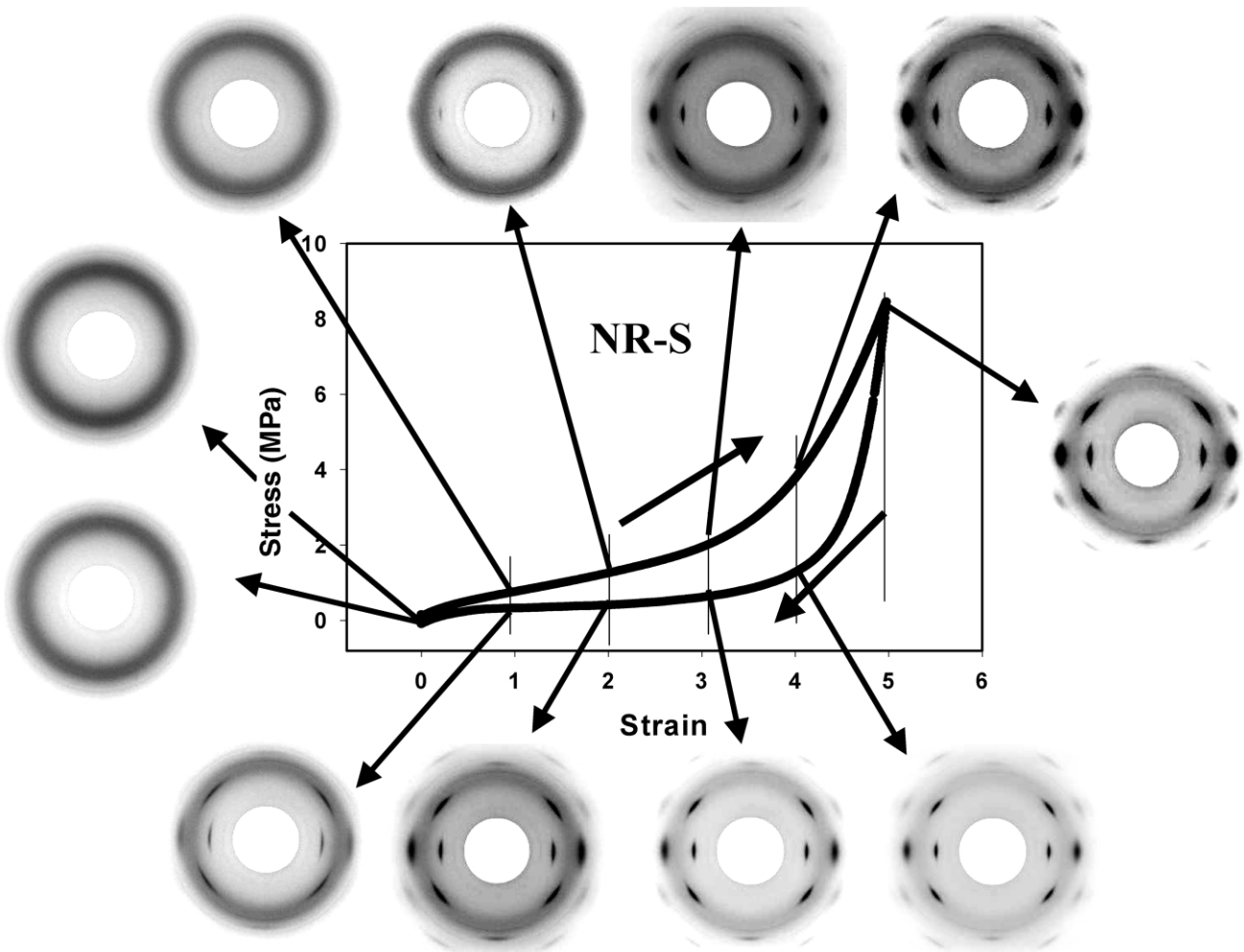

Fig. 1. The stress–strain curve and selected WAXD patterns collected during stretching and retraction of sulfur vulcanized natural rubber (NR-S) at 0 °C. Each image was taken at the average strain indicated by the arrows.

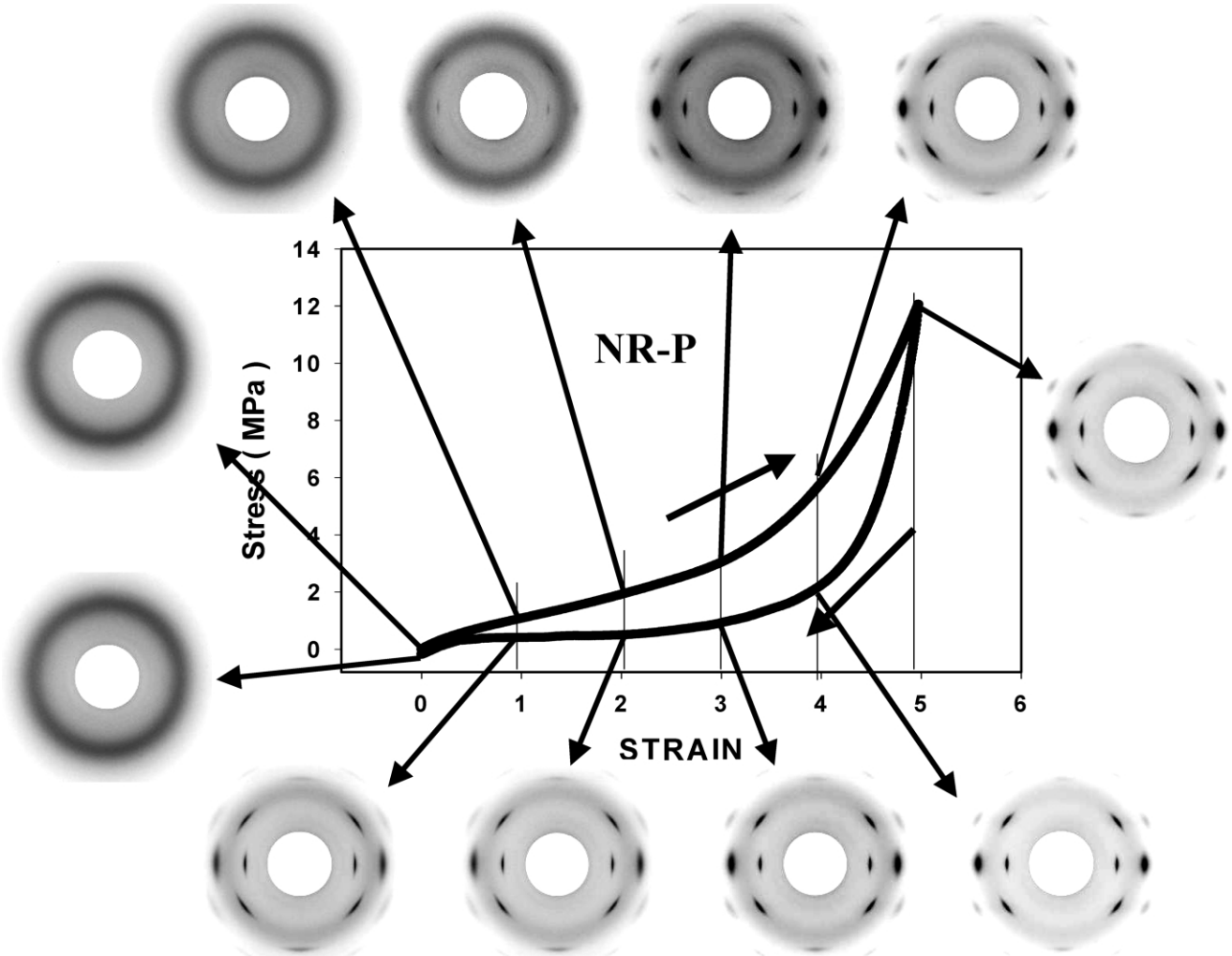

Fig. 2. The stress–strain curve and selected WAXD patterns collected during stretching and retraction of peroxide vulcanized natural rubber (NR-P) at 0 °C.

that of NR-S. When the strain returns to the zero value, crystalline reflection peaks disappear completely. In the past, NR-P was studied by Mitchell using an ordinary X-ray source [14], in which the strain-induced crystallization results seem to be identical to those observed in this study.

Time-resolved WAXD patterns and the simultaneously measured stress–strain curve of sulfur vulcanized synthetic polyisoprene (IR-S) are shown in Fig. 3. The strain-induced crystallization behavior of IR-S also resembles that of vulcanized NR (NR-S and NR-P). The attainable stress level, however, is much lower than NR. In addition, the hysteresis of the stress–strain curve in IR-S is much smaller than the one in NR. It is interesting to note that the stress during retraction in IR-S does not reach the near zero value until the strain becomes zero. The strain at which the crystallization pattern is first seen is larger, but the final crystalline pattern is about the same as the one observed in NR samples. During stretching, the stress value around strain = 3.4 in IR shows a small minimum. This phenomenon, which was attributed to the strain-induced crystallization that decreases the stress by increasing the length of the molecules along the stretching direction, has been reported and discussed recently [15,20]. In other words, the minimum stress value (around strain of 3.0) is the result of competition between the increase in stress by strain and the decrease in stress by strain-induced crystallization, which is often not too apparent. This minimum stress value that occurs before the stress upturn may represent the initiation of strain-induced crystallization [15,20]. Thus, one should pay special attention to finding the stress minimum in the stress–strain curve in order to locate the exact location of strain-induced crystallization. In the case of IR, the required strain for crystallization is rather large compared to NR. However, the final attainable degree of crystallinity is about the same. Therefore, at strains above 3.0, the crystallization rate in IR must be faster than that in NR. As a result, the minimum value in the stress curve is observed.

Mass fractions of the crystal and amorphous (oriented and unoriented) phases have been calculated by using a novel 2D image analysis method. The details of the procedures have been discussed elsewhere [17,21], and the brief description is outlined as follows. The WAXD

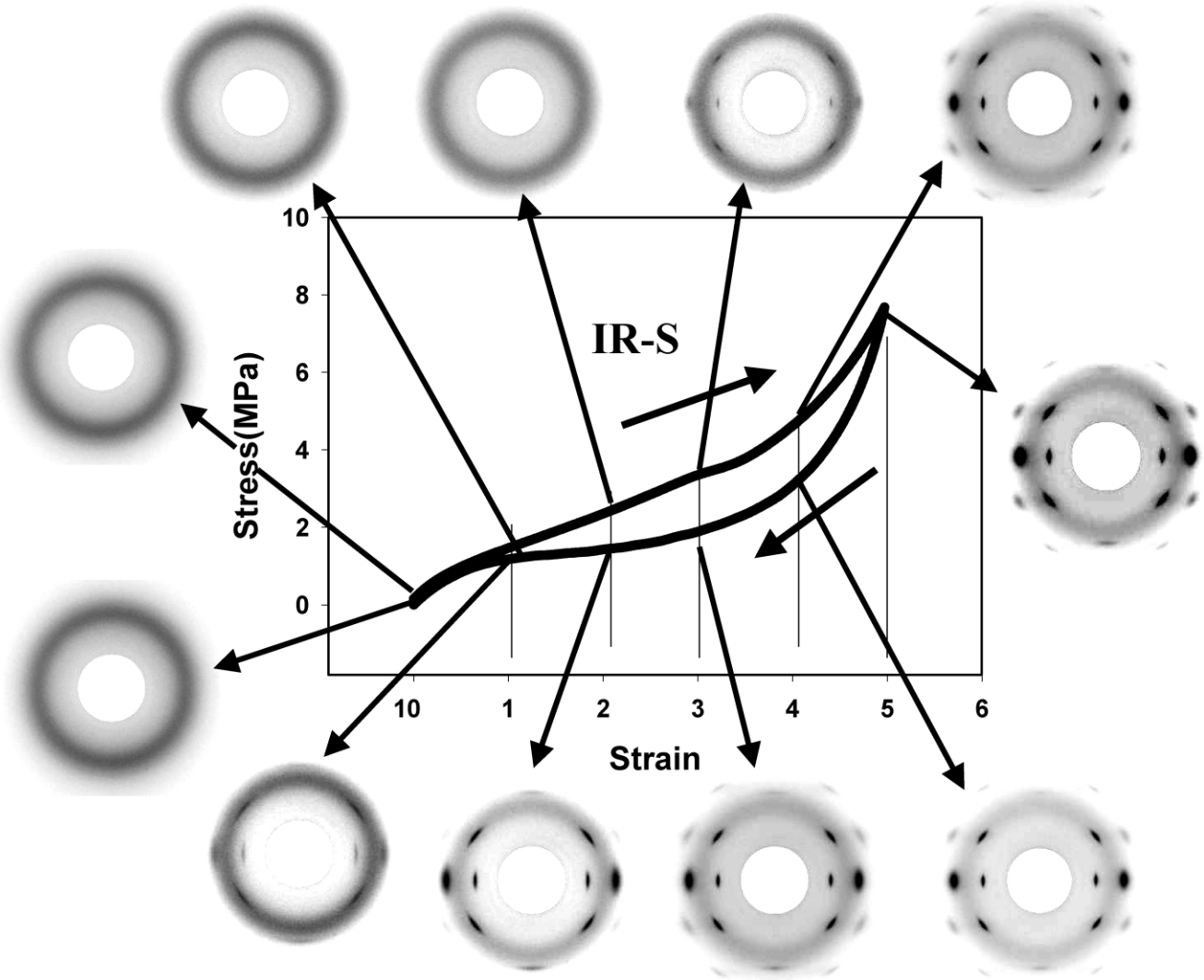

Fig. 3. The stress–strain curve and selected WAXD patterns collected during stretching and retraction of sulfur vulcanized synthetic polyisoprene rubber (IR-S) at 0 °C.

pattern taken from the unstretched sample exhibits an isotropic amorphous halo with no preferred orientation. Under deformation, the WAXD pattern shows the superposition of oriented crystal diffraction pattern and a residual amorphous halo. The isotropic and anisotropic contributions in this pattern can be de-convoluted using an analytical method as follows [21]. The isotropic contribution extracted from the WAXD pattern at the deformed state exhibits a near identical feature in the original WAXD pattern prior to stretching. The de-convoluted anisotropic contribution of the WAXD pattern is composed of oriented crystal reflection peaks and a small amount of oriented amorphous phase, which is conjugated on the equator between the strong 120 and 200 diffraction peaks. The mass fraction of the strain-induced crystals can be estimated by dividing the integration of the crystal diffraction intensity by the total scattered intensity. To acquire the total scattered intensity volume, we first transformed the data from the 2D flat-plate geometry (collected by CCD-Camera) to an undistorted geometry in the reciprocal space using the procedure described by Fraser et al. [22], and then extrapolated the data in the missing meridional region using the expansion of Legendre polynomials [23]:

$$I(s,\phi) = \sum a_{2n} P_{2n}(\cos\,\phi) \tag{1}$$

where $s = 2\sin(\theta/2)/\lambda$, ϕ represents the azimuthal angle, P_n is the Legendre polynomial of the first kind of order n and a_{2n} represents the fit coefficient. The fit functions extrapolate into the 'missing region', thereby reducing the cut-off error of the integrations.

Based on the above procedures, one can estimate the amounts of total isotropic and anisotropic mass fractions, including the unoriented amorphous fraction (ϕ_{UA}), oriented amorphous fraction (ϕ_{OA}) and oriented crystalline fraction (ϕ_{OC}). (We note that the unoriented crystalline fraction was not observed in our study.) The relationship

among the above variables can be summarized as follows:

Total molecules at the deformed state

$$= \text{isotropic fraction} + \text{anisotropic fraction} \quad (2)$$

Isotropic fraction

$$= \text{unoriented amorphous fraction } (\phi_{UA}) \quad (3)$$

Anisotropic fraction

$$= \text{oriented crystalline fraction } (\phi_{OC}) + \text{oriented} \times \text{amorphous fraction } (\phi_{OA}) \quad (4)$$

The variations of the isotropic fraction of NR-S, NR-P and IR-S at 0 °C during deformation are shown in Fig. 4. It is seen that the isotropic fraction decreases during stretching and increases during retraction, which exhibits a clear hysteresis (the level of fraction during stretching is always higher than that during retraction). This hysteresis, however, is quite different from the stress–strain relations in Figs. 1–3 in several aspects. (1) In the stress–strain curve, the stress during stretching has a higher value than the stress during retraction; the corresponding isotropic fraction during stretching is also higher than the isotropic fraction during retraction. (2) During stretching, the stress increases with strain, whereas the isotropic fraction decreases with strain. (3) During stretching, the stress–strain curves show notable differences in values and shapes, while the changes of isotropic fractions in these three vulcanized polyisoprene rubbers shows almost identical behavior (and they all reach the same value of 75% at strain 5.0). Only small differences in the recovered isotropic fraction are seen during retraction. The value of 75% in isotropic fraction at the highest strain (5.0) measured at 0 °C is the same as that measured in NR-S at strain 6.0 at 25 °C [17]. The above observations confirm that even at conditions that favor the crystallization of polyisoprene (0 °C and high strains), the majority of the molecules (75%) are still in the random coil state under large deformation.

The corresponding variations of the crystalline fraction of NR-S, NR-P and IR-S at 0 °C during deformation are shown in Fig. 5. It is found that the crystalline fraction starts to increase at strain around 2.0 in all three samples. NR-P crystallizes first, followed by NR-S and then IR-S. During retraction, the levels of crystalline fractions are significantly higher than those during stretching. The maximum amount of the crystalline fraction that can be induced by stretching is less than 20%. The amount of strain-induced crystalline fraction in NR-P is slightly larger than that in NR-S, however, a similar trend is seen in both NR samples. In other words, different vulcanization agents (sulfur versus peroxide) do not change the crystallization behavior under deformation at 0 °C. The behavior of IR under deformation is very close to that of NR. However, the onset position for crystallization and orientation in IR seems to be shifted to a larger strain as compared with NR, even though the final degree of crystallinity is about the same. This 'delay and catch up' behavior may have resulted from the linear nature of the polyisoprene chains in IR. Based on the literature [18,19], most of the molecules in NR are branched and most of the molecules in IR are linear. The branched points may exhibit the same mechanical function as the vulcanized points, where two processes can be induced by elongation. The first process involves the induction of the chain orientation between the network points, which leads to crystallization (such as formation of crystal microfibrils). The other process involves the termination of the growth of strain-induced crystallites, since the network point cannot be incorporated into the crystallites. Therefore, both branched points and vulcanization points in NR can be considered as network points. In contrast the linear chains in polyisoprene do not contain the branched points. In Fig. 5, IR-S shows the least hysteresis of strain-induced crystallization. NR-P shows the highest level of strain-induced crystalline fraction and the behavior of hysteresis. The

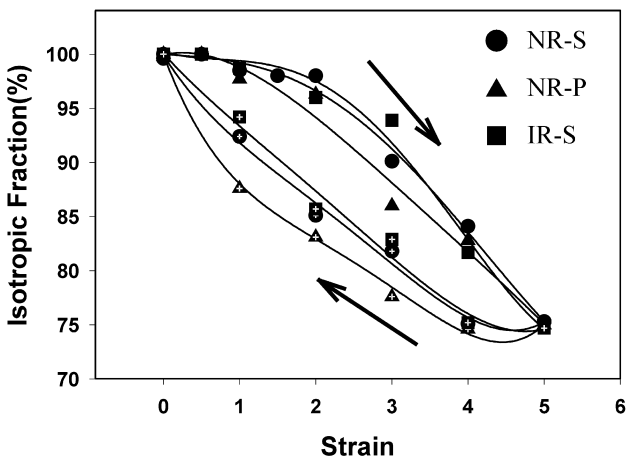

Fig. 4. The variations of the isotropic fraction of NR-S, NR-P and IR-S at 0 °C during deformation.

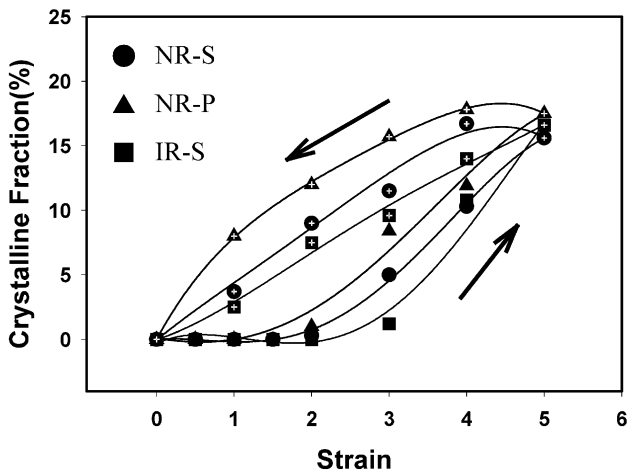

Fig. 5. The variations of the crystalline fraction of NR-S, NR-P and IR-S at 0 °C during deformation.

trends of the changes in strain-induced crystallization between the three kinds of rubbers correspond well to their levels of stress in the stress–strain curves

The variation of the oriented amorphous fraction of NR-S, NR-P and IR-S at 0 °C during deformation is shown in Fig. 6. The oriented amorphous fractions of three rubbers are significantly smaller than crystalline fraction; the average value is about 5%. The oriented amorphous fractions of them are found to increase only slightly. We thus can conclude that the increase in total anisotropic fraction is mainly due to the increase in the crystalline fraction rather than the change of the oriented amorphous fraction. It is apparent that the behavior of strain-induced crystallization dominates the total molecular orientation. We believe the oriented amorphous phase is a precursor to strain-induced crystallization in polyisoprene rubber. According to the report by Mitchell and Meier [24], the time scale needed to induce crystallites in rubber at high strain is very fast, which is in the range of 60 ms.

The above argument is also consistent with the birefringence data (Δn) of rubber under deformation [17], which is discussed as follows. Since the birefringence Δn can be expressed as [17]

$$\Delta n = \phi_{OC}\Delta n_c + \phi_{OA}\Delta n_a + \Delta n_f \quad (5)$$

where Δn_c and Δn_a represent the intrinsic birefringence of the crystalline and amorphous phases, respectively, and Δn_f is the form birefringence arising from the interphase between the crystalline and amorphous phases. The values of intrinsic birefringence of polyisoprene crystal and amorphous phase are reported to be 0.13 and 0.2, respectively [14,25]. Although the value of Δn_f depends on the applied strain because the interphase usually increases with crystallinity, we assume Δn_f to be small compared to the first and second terms (Δn_c and Δn_a). Eq. (5) thus can be simplified as:

$$\Delta n \sim \phi_{OC}\Delta n_c + \phi_{OA}\Delta n_a \quad (6)$$

The stress-optical coefficient C_o can be defined as:

$$C_o = \Delta n/\sigma \sim (\phi_{OC}\Delta n_c + \phi_{OA}\Delta n_a)/\sigma \quad (7)$$

where σ is stress. The relationships between the stress and calculated birefringence of NR-S, NR-P and IR-S during stretching at 0 °C are shown in Fig. 7. All relationships are about linear, which suggests that C_o is constant for all three samples. The constant stress-optical coefficient has been considered as the justification for the rubber elasticity theory; however, this may not be completely true. Our result indicates that the strain-induced crystallization also occurs, but this does not change the linear relationship between the stress and birefringence. In our previous study, a constant stress-optical coefficient was also observed by time-resolved birefringence measurement in natural rubber under deformation [25]. Therefore, we suggest that the increase of the strain-induced crystallinity and oriented amorphous fraction may be responsible for the increase in the birefringence of vulcanized polyisoprene rubbers under deformation, in spite of the large amount of unoriented amorphous fraction. The maximum value of birefringence of vulcanized natural rubber thus coincides with the reported experimental values that are from 0.005 to 0.035 [2,25–27]. Also, we found clear differences in stress-optical coefficients among NR-S, NR-P and IR-S. The stress-optical of IR-S is the highest, which means that molecular orientation and crystallization of IR-S contribute to its stress response much less than their counterparts of NR-S and NR-P do. This difference may come from their different network structure composed of linear (IR) and branched (NR) polyisoprene chains.

During retraction, the induced crystallinity remains high in spite of the fact that the stress decreases significantly. This can be understood by the different mechanisms in the stress and crystallization relationship during stretching and retraction. During stretching, molecules are elongated and lose freedom of movement [20]. As a result, the chains can fall into a super-cooled condition and can crystallize under the low entropy barrier. The critical strain for inducing the

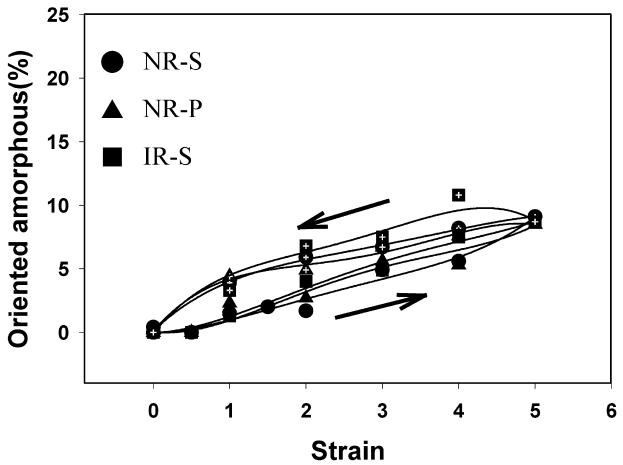

Fig. 6. The variations of the oriented amorphous fraction of NR-S, NR-P and IR-S at 0 °C during deformation.

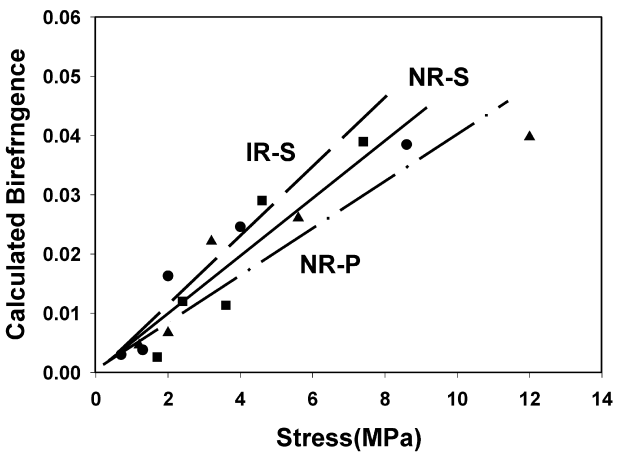

Fig. 7. The calculated birefringence and stress relationship of NR-S, NR-P and IR-S during stretching at 0 °C.

crystallization will depend on the stretching speed [28]. In other words, there is a competition between the rate of crystallization and the rate of stretching. When the rate of stretching is larger than the rate of crystallization, no strain-induced crystallinity can be obtained. However, once the crystallinity is formed, these crystallites could acquire certain thermal stability. This is seen in the process of retraction, where the strain-induced crystallites do not melt immediately. Furthermore, we noticed that the stress–strain curve during retraction does not noticeably depend on the rate of stretching [28]. The relationship seems to depend on strain and temperature only.

Based on the above results from three different types of vulcanized rubber samples, our previously proposed concept for strain-induced crystallization in natural rubber [17] is still correct and applicable to all the samples studied. The schematic diagram of strain-induced crystallization in nature or synthetic rubber is illustrated in Fig. 8. To contrast the difference between the 'ideal' rubber and the 'real' rubber, a homogeneous cross-link network and its deformed state is also illustrated. The ideal network model consists of the same length of molecules between the network points. It is generally assumed that all of the molecules between the network points deform similarly under an affine deformation assumption. This model, however, is not consistent with the observation of the persistently large amorphous fraction at high strains. The real network in vulcanized rubber is composed of molecules with lengths of broad distribution between the network points. Under stretching, only the molecules of smaller length between the network points are deformed and the molecules of much longer lengths remain in the random coil state. This model is consistent with the observation of a large fraction of amorphous phase at high strains in this study.

The heterogeneity of the cross-link distribution in vulcanized polyisoprene rubber results in inhomogeneous arrangements of phases in stretched rubber [29,30]. The resultant structures under deformation include highly oriented crystallites between the network points, oriented amorphous phase and random coil amorphous chains as the major matrix. The crystallites between the network points contain a microfibrillar structure, which has also been verified by small-angle X-ray scattering (SAXS, results to be discussed elsewhere). This microfibrillar structure should function as a stronger network point than the multiple chemical bonds in the pure chemical network structure. This may be the reason why polyisoprene rubber is stronger than other vulcanized rubbers that cannot be crystallized under stretching. Although strain-induced crystallization itself does not increase the stress (it actually decreases the stress slightly), the crystallization creates the microfibrillar network structure that is able to increase the elongation at break since the stronger network points endure the high strain. As a result, the tensile strength is increased.

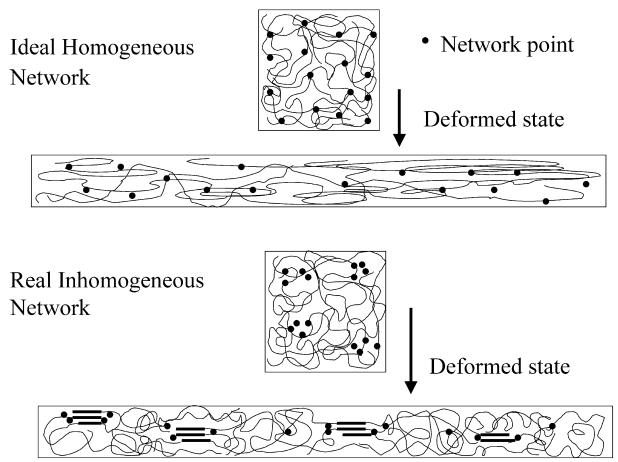

Fig. 8. Schematic model of uniaxial deformed vulcanized polyisoprene. Undeformed ideal network, deformed ideal network, undeformed real network and deformed real network (microfibrillar structure, crystallites, network points and random coils).

4. Conclusions

An in situ synchrotron X-ray diffraction study of three kinds of vulcanized polyisoprene rubber samples during uniaxial deformation at 0 °C revealed that the majority of molecules (up to 75% of the mass) remain unoriented amorphous polymers even at large strains. The fraction of the strain-induced crystallites at high strains is about 20%, where the corresponding fraction of the oriented amorphous phase is about 5%. The behavior is an intrinsic property of vulcanized polyisoprene since different vulcanization agents, different modulus levels and different stereoregularity of polyisoprene chains do not affect the behavior of molecular orientation and induced crystallization significantly. Synthetic polyisoprene shows a delay and catch up behavior in strain-induced crystallization compared to natural rubber. The constant stress-optical coefficient, is not due to the affine deformation of ideal network, but can be explained by the contributions of strain-induced crystalline structures and oriented amorphous fractions. The strain-induced crystallites with a microfibrillar structure between the network points are responsible for the high tensile strength of polyisoprene rubbers.

Acknowledgements

We thank Professor A.N. Gent of the University of Akron for supplying peroxide vulcanized natural rubber and for giving us the permission to publish the data from this sample. The financial support of this study was provided by the National Science Foundation (DMR-0098104).

References

[1] Flory PJ. Principles of polymer chemistry. Cornell: Cornell University Press; 1953.
[2] Treloar RG. The physics of rubber elasticity, 3rd ed. Oxford: Oxford University Press; 1975.
[3] Treloar RG. Trans Faraday Soc 1947;43:277. See also p. 284.
[4] Flory PJ. J Chem Phys 1947;15:397.
[5] Gent AN. Trans Faraday Soc 1954;50:521.
[6] Magill JH. Rubber Chem Technol 1995;68:507.
[7] Phillips PJ. Rep Progress Phys 1990;53:549.
[8] Stein RS. Rubber Chem Technol 1976;49:458.
[9] Shimomura Y, White JL. J Appl Polym Sci 1982;27:3553.
[10] Gehman SD, Field JE. J Appl Phys 1939;10:564.
[11] Gehman SD, Field JE. J Appl Phys 1944;15:371.
[12] Bunn CW. Proc R Soc A 1942;180:40.
[13] Luch D, Yeh GSY. J Macromol Sci 1973;B7(1):121.
[14] Mitchell GR. Polymer 1984;25:1562.
[15] Toki S, Fujimaki T, Okuyama M. Polymer 2000;41:5423.
[16] Murakami S, Senoo K, Toki S, Kohjiya S. Polymer 2002;43:2117.
[17] Toki S, Sics I, Ran S, Liu L, Hsiao BS, Murakami S, Senoo K, Kohjiya S. Macromolecules 2002;35:6578.
[18] Tanaka Y. Rubber Chem Technol 2001;74:355.
[19] Kawahara S, Eng AH. J Soc Rubber Ind Jpn 2002;73:627.
[20] Miyamoto Y, Yamao H, Sekimoto K. International Symposium on Polymer Crystallization, Mishima, Japan, June; 2002.
[21] Ran S, Fang D, Zong X, Hsiao BS, Chu B, Cunniff PM. Polymer 2001; 42:1601.
[22] Fraser RDB, Marae TP, Miller A, Rowlands RJ. J Appl Crystallogr 1976;9:81.
[23] Ruland W. Colloid Polym Sci 1977;255:833.
[24] Mitchell JC, Meier DJ. J Polym Sci 1968;A-2(6):1689.
[25] Hashiyama M, Gaylord R, Stein RS. Macromol Chem Suppl 1975;1: 579.
[26] Toki S, Sen TZ, Valladares D, Cakmak M. ACS Rubber Div Spring Meeting. Paper No. 12; 2001.
[27] Choi IS, Roland CM. Rubber Chem Technol 1997;70:202.
[28] Miyamoto Y, Fukao K, Yamao H, Sekimoto K. Phys Rev Lett 2002; 88:225504.
[29] Goritzs D, Grassler R. Rubber Chem Technol 1987;60:217.
[30] Reichert WF, Goritzs D. Rubber Chem Technol 1992;66:1.